Electronic Materials Letters, Vol. 1, No. 2 (2005), pp. 00-00

Improvement of the Electrical Properties of Al-Based Reflective Electrode on P-Type GaN for Flip-Chip Light-Emitting Diodes

Dong-Seok Leem, Takhee Lee and Tae-Yeon Seong*,[1]

Department of Materials Science and Engineering, Gwangju Institute of Science and
Technology (GIST), Gwangju 500-712, Korea
[1]Department of Materials Science and Engineering, Korea University, Seoul 136-701, Korea

We report on the formation of Ag/TiN$_x$/Al contacts to *p*-type GaN for flip-chip light- emitting diodes (LEDs). The Ag/TiN$_x$/Al contact exhibits linear *I-V* behavior with a specific contact resistance of 4.4×10^{-3} Ωcm^2 after annealing at 430 °C for 1 min in nitrogen ambient. It is shown that the continuous Ag interlayer is broken into Ag nano-dots when annealed. It is also demonstrated that the TiN$_x$ barrier layer effectively hampers the indiffusion of Al toward GaN. Blue LEDs are fabricated using the annealed Ag/TiN$_x$/Al contacts and are compared with those made with annealed Ni/Au/Al contacts.

Keywords: ohmic contacts, GaN, TiN barrier layer, flip-chip light-emitting diodes, Al reflector

1. INTRODUCTION

Nitride-based semiconductors are of great technological importance for the fabrication of high-brightness blue and ultraviolet light-emitting diodes (LEDs). Recent research on nitride-based LEDs has been directed toward solid-state lighting applications[1]. For the realization of solid-state lighting, high light extraction efficiency of LEDs is essential. In order to improve light extraction efficiency, and hence enhance device performance, LEDs with flip-chip geometry have been introduced[2,3]. In the flip-chip configuration, LEDs are fabricated with reflective *p*-type electrodes such as Ag and Al layers[4-7]. Among these, Ag layers are commonly used since they give high reflectivity and good ohmic behavior to *p*-GaN[1]. However, the Ag reflector has drawbacks such as poor adhesion to *p*-GaN and thermal instability[4,7]. Al electrodes have good thermal stability and reflectivity, comparable to that of Ag reflectors. However, Al reflectors have not been widely used because they produce poor ohmic contacts on *p*-GaN. Thus, instead of single Al layers, Al-based multilayers with Ni or Ni/Au contact layers have been used to improve ohmic behavior, but the electrical property of the contacts remains unsatisfactory[1,7]. Titanium nitride (TiN$_x$) is known to be one of the best diffusion barriers for electronic devices[8,9]. TiN$_x$ was also used as a contact layer for optoelectronic devices, because of its low resistivity and high transparency[10,11]. In this work, we have investigated Al-based reflective contacts to *p*-GaN using Ag interlayers and TiN$_x$ barrier layers. The Ag/TiN$_x$/Al contacts became good ohmic with a specific contact resistance of 4.4×10^{-3} Ωcm^2 when annealed at 430 °C for 1 min in nitrogen ambient. LEDs fabricated with the annealed Ag/TiN$_x$/Al *p*-GaN contact layers yield better electrical behavior than those with the commonly used Ni/Au/Al contacts.

2. EXPERIMENT

1.5 m-thick *p*-type GaN: Mg layers (4×10^{17} cm^{-3}), grown by metal-organic chemical vapor deposition, were ultrasonically degreased using trichloro-ethylene, acetone, methanol, and DI water for 5 min in each step, followed by N2 blowing. Prior to photolithography, the samples were treated with a buffered oxide etch (BOE) solution for 20 min and rinsed in DI water. Circular transmission line method (CTLM) patterns were defined on *p*-type GaN by standard photolithography and a lift-off technique for measuring specific contact resistance[12]. The outer dot radius was fixed to be 75 μm and the spacing between the inner and outer radii varied from 4 to 25 μm. After the BOE treatment, Ag (2.5 nm) and TiN$_x$ (30-50 nm) layers were deposited at room temperature by electron beam evaporation. Prior to the deposition of 200 nm-thick Al layers, the Ag/TiN$_x$ samples were kept in air at room temperature for 10 h in order to introduce oxygen into TiN$_x$ grain boundaries[8]. For comparison, Ni(2.5 nm)/Au(2.5 nm)/Al(200 nm) layers, which are commonly used for flip-

---

*Corresponding author: tyseong@korea.ac.kr

chip LEDs, were also deposited by electron beam evaporation. In addition, Ag (2.5 nm)/Al (200 nm) and TiN_x/(50 nm)/Al(200 nm) schemes were also deposited. Some of the samples were then rapid-thermal-annealed at 430 °C for 1 min in nitrogen ambient. Current-voltage (*I-V*) measurements were performed using a parameter analyzer (HP 4155A). The interfacial reaction products were characterized by glancing angle X-ray diffraction (GXRD: a Rigaku diffractometer (D/MAX-RC)) (using Cu Kα radiation). The microstructure was characterized by transmission electron microscopy (TEM, JEOL 2010) operated at 200 kV.

3. RESULTS AND DISCUSSION

Figure 1 shows the typical *I-V* characteristics of Ni/Au/Al, Ag/TiN_x(50 nm)/Al, and Ag/Al contacts before and after annealing at 430 °C in nitrogen ambient, respectively, measured on 4 μm-spaced metal pads. For the as-deposited samples (Fig. 1(a)), the Ag/Al contact displayed rectifying behavior whereas Ni/Au/Al and Ag/TiN_x/Al contacts exhibited near-linear *I-V* behavior. For the annealed samples (Fig. 1(b)), the Ag/Al contact still exhibited poor *I-V* behaviors. Furthermore, the Ni/Au/Al contact showed considerable degradation of its electrical characteristic after annealing. However, for the Ag/TiN_x/Al contact, the *I-V* behavior was somewhat improved upon annealing, indicating that the introduction of TiN_x layer serves as an effective diffusion barrier layer. Specific contact resistance was determined from the plots of the measured resistances versus the spacing between the CTLM pads[12]. The least-square method was used to fit a straight line to the experimental data. Measurement showed that the annealed Ag/TiN_x/Al contact gives a contact resistivity of 4.4×10^{-3} Ωcm^2.

Figure 2(a) shows a cross-sectional TEM image of an Ag/TiN_x(50 nm)/Al contact annealed at 430 °C. The Al and TiN_x layers were well-defined even after annealing. Notably, the continuous Ag layer was broken up into nano-dots (7-13 nm in size) at the TiN_x/GaN interface, as shown in the high-resolution TEM image of Fig. 2(b). In order to investigate possible interfacial reactions between the metal layers and GaN, an AES analysis (not shown) of the Ag/TiN_x(50 nm)/Al contact was conducted. For the as-deposited sample, individual Al and TiN_x layers were well defined and an oxygen layer was also detected through the TiN_x layer. The formation of the oxygen layer is due to exposure of the sample in air before deposition of the Al layer. For the annealed sample, a small amount of Al diffused into the TiN_x layer. However, it did not penetrate deeply to the GaN layer. It is also shown that some amount of Ga outdiffused into the Ag/TiN_x layer. This indicates the possible formation of a Ga-Ag solid solution[13,14].

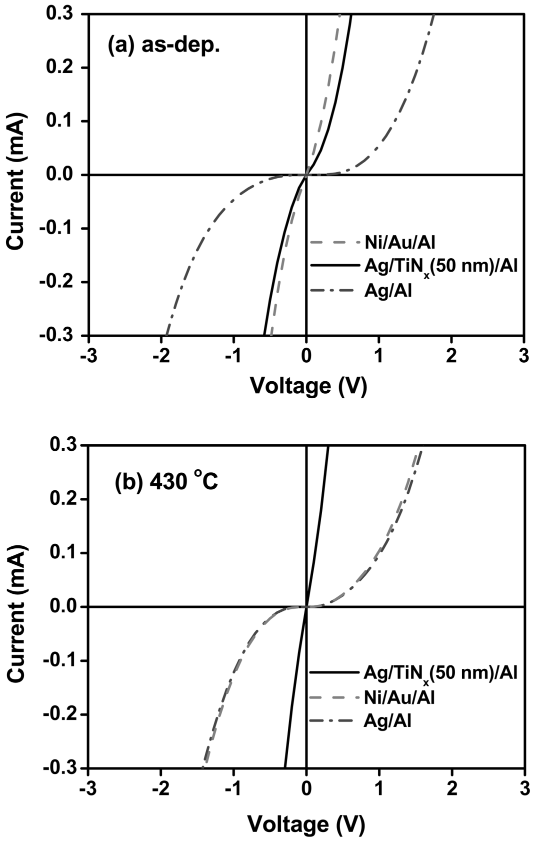

Fig. 1. Typical *I-V* characteristics of the Ni/Au/Al, Ag/TiN_x/Al, and Ag/Al contacts (a) before and (b) after annealing at 430 °C for 1 min in nitrogen ambient.

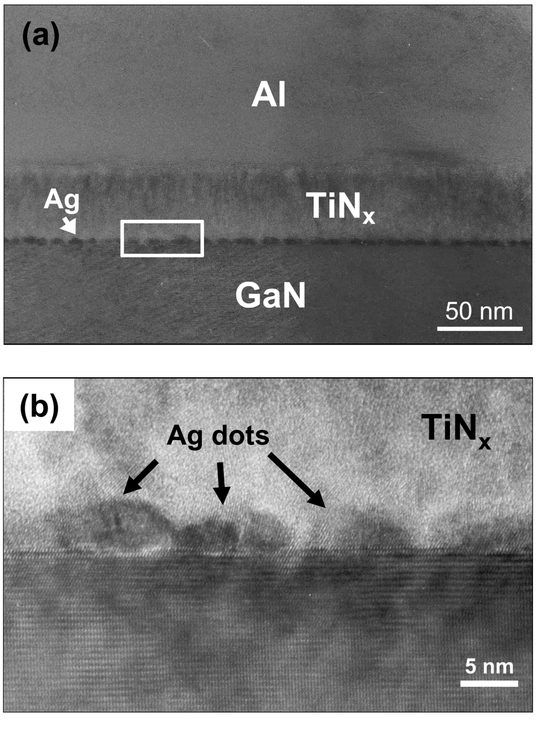

Fig. 2. (a) Cross-sectional TEM image of the Ag/TiN_x/Al contact annealed at 430 °C. (b) HRTEM image of the sample.

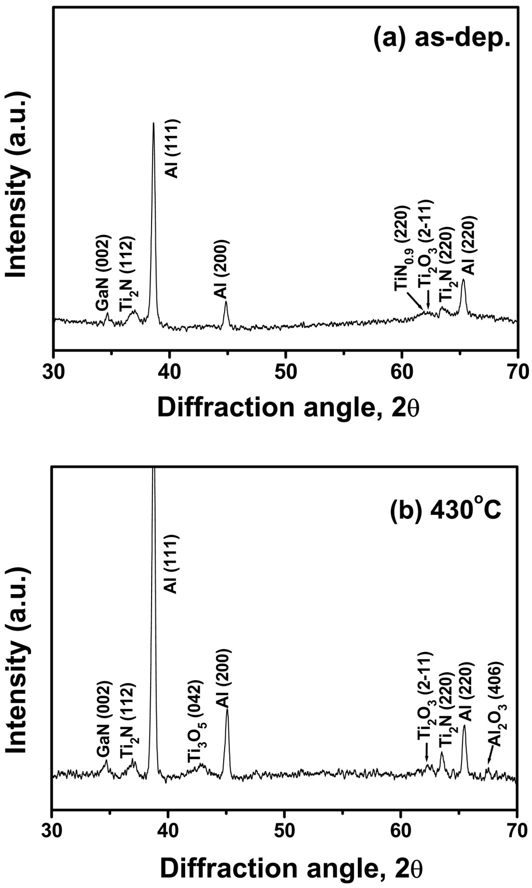

Fig. 3. Glancing XRD plots of the Ag/TiN_x/Al contacts (a) before and (b) after annealing at 430 °C.

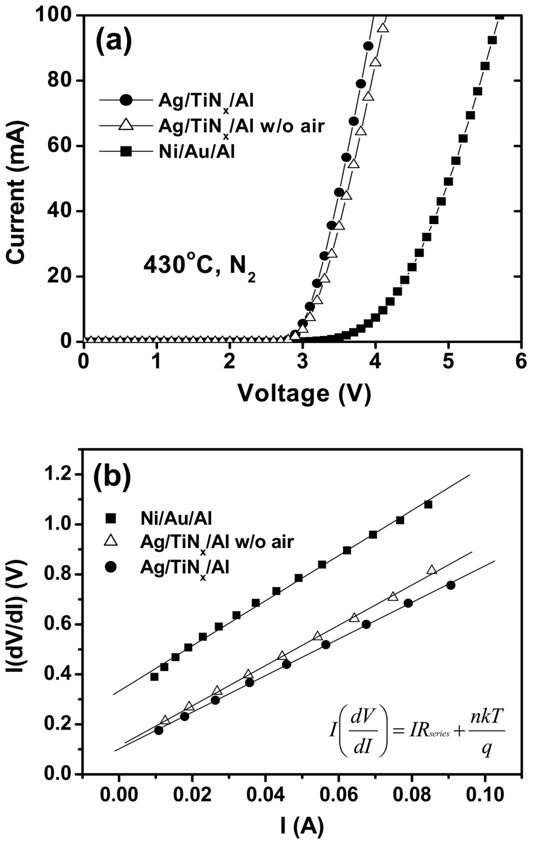

Fig. 4. (a) Typical *I-V* characteristics of GaN blue LEDs fabricated with the Ag/TiN_x/Al, Ag/TiN_x/Al without air exposure on TiN_x layer, and Ni/Au/Al contacts annealed at 430 °C. (b) Plot and linear fitting of the series resistance calculated from the LED *I-V* curves.

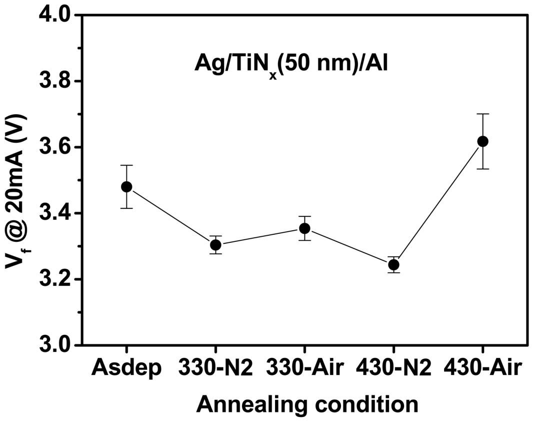

Fig. 5. The variation of forward-bias voltages of the GaN blue LEDs fabricated with the Ag/TiN_x/Al contacts depending on the annealing conditions.

Figure 3 shows GXRD results obtained from the Ag/TiN_x(50 nm)/Al contact before and after annealing at 430 °C. For the as-deposited sample (Fig. 3(a)), in addition to Al, there are nitrogen deficient phases, such as Ti_2N and $TiN_{0.9}$. A very small amount of Ti-oxide phase, such as Ti_2O_3, was also detected; its presence is attributed to exposure of the sample to air before deposition of the Al layer. For the annealed sample (Fig. 3(b)), in addition to the Ti_2N phase, Ti-oxide phases, such as Ti_2O_3 and Ti_3O_5, are formed. However, Ag was not detected in either sample, as most of the Ag peaks overlap with the Al peaks.

InGaN/GaN multi-quantum-well blue LEDs (450 nm) were fabricated using Ag/TiN_x(50 nm)/Al and Ni/Au/Al contact layers annealed at 430 °C and their performances were characterized, as shown in Figs. 4(a) and (b). LEDs with a Ni/Au/Al layer give considerably higher forward-bias voltages of 4.43 ± 0.12 V at 20 mA, whereas LEDs made with the Ag/TiN_x/Al contact layer show forward-bias voltages of 3.24 ± 0.02 V at an injection current of 20 mA, as shown in Fig. 4(a). These results are in good agreement with their *I-V* behaviours (Fig. 1(b)). In order to investigate whether exposure of the Ag/TiN_x layer to air can effectively improve device performance, a Ag/TiN_x(50 nm)/Al contact layer without air exposure on the TiN_x layer before Al deposition was prepared. LEDs with this contact displayed slightly higher forward-bias voltages (3.30 ± 0.03 V at 20 mA) than the LED with the Ag/TiN_x/Al contact, indicating

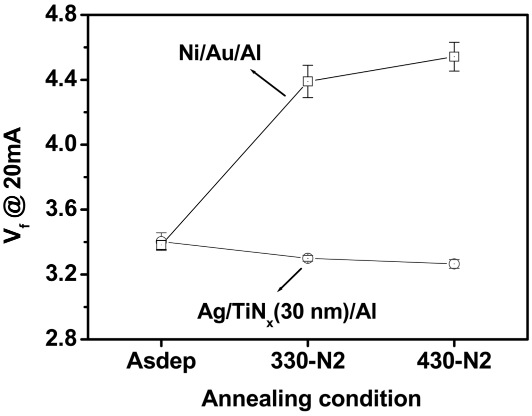

Fig. 6. The variation of forward-bias voltages of the GaN blue LEDs with the Ag/TiN$_x$(30 nm)/Al contacts depending on the annealing temperature.

air exposure on the TiN$_x$ layer is an effective method to further enhance the electrical property of the contacts. The series resistance of LEDs can be represented by the slope (Rseries) of *I(dV/dI)* versus *I* curve, as shown in Fig. 4(b). The LED with the Ni/Au/Al contact exhibited a series resistance of 9.03 Ω, whereas the LEDs with the Ag/TiN$_x$/Al contact layer with and without air exposure on the TiN$_x$ layer give a relatively low series resistance of 7.32 and 8.06 Ω, respectively.

Figure 5 shows the variation of forward-bias voltages of LEDs fabricated with the Ag/TiN$_x$(50 nm)/Al contact layer depending on the annealing conditions. The LEDs with the Ag/TiN$_x$/Al contact annealed in nitrogen ambient exhibited relatively lower forward-bias voltages compared to the LEDs with the Ag/TiN$_x$/Al layer annealed in air ambient.

In order to determine the effective TiN$_x$ barrier layer thickness, we reduced the thickness of the TiN$_x$ layer. The LEDs made with Ag/TiN$_x$(30 nm)/Al contacts annealed at 430 ^{o}C exhibited forward-bais voltages of 3.27 ± 0.03 V at 20 ± mA, as shown in Fig. 6. This indicates that a TiN$_x$ layer thickness of 30 nm is effective in terms of obtaining contacts having a good electrical property.

Unlike the non-linear *I-V* behaviours of Ni/Au/Al contacts upon annealing, the Ag/TiN$_x$/Al contact layer displayed relatively good ohmic behavior after annealing. This behavior could be explained as follows. First, the improvement of the electrical property of the contact can be related to the formation of Ag nano-dots at the TiN$_x$/GaN interface, as shown in the TEM results. The An nano-dots(?) lead to the formation of inhomogeneous Schottky barriers at the interface. According to the electronic transport theory, at a metal-semiconductor interface with an inhomogeneous Schottky barriers[16], the difference between the SBHs of Ag/GaN and TiN$_x$/GaN and the size effect of the nano-scale Ag dots could result in an increase of the electric field at the interface. This would result in a lowering of the barrier height and a consequent reduction of the contact resistivity[15,16]. Second, the outdiffusion of Ga caused by the formation of Ag-Ga solid solution[13,14] results in the generation of deep acceptor-like Ga vacancies near the GaN surface and hence an increase in carrier concentration[17]. Indeed, we demonstrated the *I-V* characteristic of the TiN$_x$/Al contact layer (not shown). It should be noted that the contact revealed a rectifying *I-V* behavior, implying that the Ag interlayer plays an important role in forming ohmic contacts. Finally, the TiN$_x$ barrier layer effectively suppresses the indiffusion of Al toward GaN. In general, Al indiffusion could cause the formation of Al-nitride phases, generating donor-like nitrogen vacancies near the GaN surface, which is detrimental to *p*-type GaN ohmic formation. Moreover, Ti-oxide phases formed on the TiN$_x$ layer due to air exposure on the Ag/TiN$_x$ layer could segregate along the TiN$_x$ grain boundaries and thus could hamper the diffusion of Al through the TiN$_x$ film by grain boundary diffusion[9].

4. CONCLUSION

In this work, Ag/TiN$_x$/Al contacts were studied with respect to the formation of ohmic contacts to *p*-GaN for flip-chip LEDs. The contacts produced ohmic behaviour with a specific contact resistance of 4.4×10^{-3} $\Omega\mathrm{cm}^2$ when annealed at 430 ^{o}C for in nitrogen ambient, which is much better than that of the commonly used Ni/Au/Al contacts. It was shown that the use of TiN$_x$ barrier layers is effective in hindering indiffusion of Al toward GaN, and hence facilitates *p*-type ohmic formation. Moreover, the exposure of Ag/TiN$_x$ layers to air is also an effective method to protect against Al indiffusion. Based on TEM, GXRD, and AES results, the ohmic formation was attributed to the combined effects of the formation of Ag nano-dots, an Ag-Ga solid solution, and TiN$_x$ barrier layers. Blue LEDs fabricated with the annealed Ag/TiN$_x$/Al *p*-type contacts showed forward-bias voltage of 3.24 V at 20 mA, while LEDs with annealed Ni/Au/Al contacts yielded a forward-bias voltage of 4.43 V at 20 mA.

REFERENCES

1. D. A. Steigerwald, J. C. Bhat, D. Collins, R. M. Fletcher, M. O. Holcomb, M, J. Ludowise, P. S. Martin, and S. L. Rudaz, *IEEE J. Sel. Top. Quantum Electron.* **8**, 310 (2002).
2. J. J. Wierer, D. A. Steigerwald, M. R. Krames, J. J. O'Shea, M. J. Ludowise, G. Christenson, Y.-C. Shen, C. Lowery, P. S. Martin, S. Subramanya, W. Gotz, N. F. Gardner, R. S. Kern, and S. A. Stockman, *Appl. Phys. Lett.* **78**, 3379 (2001).
3. M. Koike, N. Shibata, H. Kato, and Y. Takahashi, *IEEE J. Sel. Top. Quantum Electron.* **8**, 271 (2002).
4. D. L. Hibbard, S. P. Jung, C. Wang, D. Ullery, Y. S. Zhao, H. P. Lee, W. So, and H. Liu, *Appl. Phys. Lett.* **83**, 311 (2003).

5. J.-O. Song, D.-S. Leem, J. S. Kwak, O. H. Nam, Y. Park, and T.-Y. Seong, Appl. Phys. Lett. 83, 4990 (2003).
6. H. W. Jang and J.-L. Lee, *Appl. Phys. Lett.* **85**, 4421 (2004).
7. H. S. Venugopalan, X. Gao, T. Zhang, B. S. Shelton, A. Dicarlo, I. Eliashevich, and M. Hsing, *Proc. of SPIE* **5187**, 260 (2004).
8. W. Sinke, G. P. A. Frijink, and F. W. Saris, *Appl. Phys. Lett.* **47**, 471 (1985).
9. V. Fortin, S. C. Gujrathi, G. Gagnon, R. Gauvin, J. F. Currie, L. Ouellet, and Y. Tremblay, *J. Vac. Sci. Technol. B* **17**, 423 (1999).
10. Y.-Z. Chiou, Y.-K. Su, S.-J. Chang, J. F. Chen, C.-S. Chang, S.-H. Liu, Y.-C. Lin, and C.-H. Chen, *Jpn. J. Appl. Phys.* **41**, 3643 (2002).
11. C.-C. Liu, W.-T. Wang, M.-P. Houng, Y.-H. Wang, *Jpn. J. Appl. Phys.* **43**, 594 (2004).
12. G. S. Marlow and M. B. Das, *Solid-State Electron.* **25**, 91 (1982).
13. A. E. Gunnes, O. B. Karlsen, A. Olsen and P. T. Zagierski, *J. Alloy Compounds* **297**, 144 (2000).
14. J.-O. Song, J. S. Kwak, Y. Park, and T.-Y. Seong, *Appl. Phys. Lett.* **86**, 062104 (2005).
15. R. T. Tung, *Phys. Rev. B* **45**, 13509 (1992).
16. J. I. Sohn, J.-O Song, D.-S. Leem, S. Lee, and T.-Y. Seong, *Electrochem. Solid-State Lett*. **7**, G179 (2004).
17. V. M. Bermudez, D. D. Koleske, and A. E. Wickenden, *Appl. Surf. Sci.* **126**, 69 (1998).